

## Draft SPOTS Standard Part III (1)



### CALIBRATION AND ASSESSMENT OF OPTICAL STRAIN MEASUREMENTS

---

---

## Good Practice Guide to Geometric Moiré for In-plane Displacement/Strain Analysis

December 2005



## 1. Scope

Geometric moiré is a technique of experimental full field and non-contact in-plane displacement measurement and strain analysis. It relies simply on the comparison between a deformed grid attached to the specimen under load and an undeformed master grid used as a length standard to establish displacement and strain. The moiré fringes which are monitored as an intensity pattern with a CDD camera provide full-field information about in-plane displacement vectors (in x and y directions) when the master grid is placed vertically or horizontally with respect to the crossed specimen grid. The displacement fields are numerically differentiated in order to obtain strain maps.

From the physical point of view, geometric moiré is based on the superposition of deformed and master grids, white light illumination, use of a CCD camera, and monitoring of the change of the optical phase in moiré fringes due to displacements.

## 2. Reference materials

### ISO Norms

ISO/TAG4/WG3, “Guide to the Expression of Uncertainty in Measurements (GUM), 1995, identical with EN130005: 1999: “Guide to expression of Uncertainty in Measurement”

ISO IEC 17025:1999: “General requirements for the competence of testing and calibration laboratories”

ISO 10012:2003: “Measurement Management Systems- requirements for measurement processes and measuring equipment”

### ASTM Standards

E 2208-02 Standard Guide for Evaluating Non-Contacting Optical Strain Measurement Systems.

### Technical notes

TN-703: Geometric moiré of strain analysis, Vishay Measurement Group Inc., Raleigh NC., (1977).

### Other

VDI/VDE 2634 - Practical acceptance & verification methods for the evaluation of accuracy.



### 3. Symbols and abbreviations

Symbol	Definition	Units
$a(x,y)$	background intensity,	$W/m^2$
$b(x,y)$	contrast of the fringes,	$W/m^2$
$d_x, d_y$	standard linear distance,	m
$f_{ox}, f_{oy}$	spatial carrier frequency in the $x$ or $y$ direction,	1/m
$f_d$	sampling frequency of the detector,	1/m
$I(x,y)$	intensity distribution,	$W/m^2$
$I_m(x,y)$	intensity of moiré fringes,	$W/m^2$
$k, b_1, b_2, \dots, b_k$	profile of the moiré fringes,	
$k_x, k_y$	actual number of pixels for standard linear distance,	-
$n$	half the number of pixels over which differentiation is performed	-
$M$	an integer	-
$N(x,y)$	integer number of the fringe at the point $(x,y)$ in the domain,	-
$p$	pitch (distance between lines) of the specimen grid,	m
$u(x,y), v(x,y)$	displacement in directions $x$ and $y$ respectively,	m
$\alpha$	shift angle of the fringes,	rad
$\beta_x, \beta_y$	imaging system magnification,	-
$\Delta x, \Delta y$	distance between pixels at CCD matrix plane,	m
$\varepsilon_x, \varepsilon_y, \gamma_{xy}$	strain components referred to $x$ - $y$ rectangular coordinates,	m/m, %, $\mu S$
$\phi(x,y)$	unwrapped phase	rad
$\varphi$	phase shift between frames or sampling points	rad

#### Abbreviations

CCD	- Couple Charge Device
CMOS	- Complementary Metal-Oxide Semiconductor
FT (FFT)	- Fourier Transform (Fast Fourier Transform)
RG	- reference grille/grid
RMS	- Root Mean Square
SCPS	- Spatial Carrier Phase Shifting
SG	- specimen grid
TPS	- Temporal Phase Shifting

### 4. Terminology

*fringe pattern analysis* - techniques for conversion of the intensity distribution at an output of a device producing a fringe pattern in space, into a continuous phase map representing the unambiguous difference of phase between the two interfering beams or superimposed structures at any point at the output space.

*moiré phenomenon* - the phenomenon which can be readily observed when superimposing two periodic or quasiperiodic structures.



- moiré fringe pattern* - fringe pattern which is formed when two structures with the same or slightly different line spacing are set approximately parallel. The spacing and orientation of the moiré fringes depend on the spacing and orientation of the structures being overlapped. The visibility of fringes is related to the width of transparent or black lines with respect to the line spacing of the structures.
- specimen grid* - cross-type grid with two component linear perpendicular grilles with the same spatial frequency.
- master grille* - linear grille, usually binary and with equal width of opaque and transparent lines.

## 5. Principles of the method

### 5.1. Introduction

A moiré fringe pattern results when two sets of closely spaced lines are superimposed, and can be observed with transmitted or reflected light; some light areas will be viewed when lines of one set coincide with the other, and dark areas will appear when the lines of one set coincide with spaces between the lines of the other.

The moiré fringe phenomenon is used in strain analysis as an experimental method to determine the components of displacement ( $u$ ,  $v$ ) or strains ( $\varepsilon_x$ ,  $\varepsilon_y$ ) on a part subjected to load. The moiré fringe technique can be employed to measure displacement or strain, regardless of strain magnitude, specimen temperature, testing time, test frequency, or speed.

While the grid itself is composed of 1 to 100 lines per mm, usually not visible, the pattern of moiré fringes has the frequency of the lowest beat frequency component and therefore it is easily observed or captured by a camera for analysis. Geometric moiré is, in fact, simply the comparison between a specimen grid deformed due to load and an undeformed master grid used as a length standard, to establish displacement and strain.

### 5.2 Basic principles for planar strain state

When a body is subjected to loads, strains produce displacement. In an arbitrary system of coordinates  $x$ ,  $y$ , the basic components of displacement of a point in directions  $x$  and  $y$  are usually designated  $u$  and  $v$ , respectively. Also, the elongation (strain) changes the distance between points on the body. The strains are related to displacements by well known formulae of stress analysis (see also Figure 1):

$$\varepsilon_x = \frac{\partial u}{\partial x} \quad \varepsilon_y = \frac{\partial v}{\partial y} \quad \gamma_{xy} = \frac{\partial u}{\partial x} + \frac{\partial v}{\partial y} \quad (1)$$

$\varepsilon_x$ ,  $\varepsilon_y$ ,  $\gamma_{xy}$  are strain components referred to  $x$ - $y$  rectangular coordinates, and  $u(x,y)$ ,  $v(x,y)$  are displacement in directions  $x$  and  $y$ , respectively.



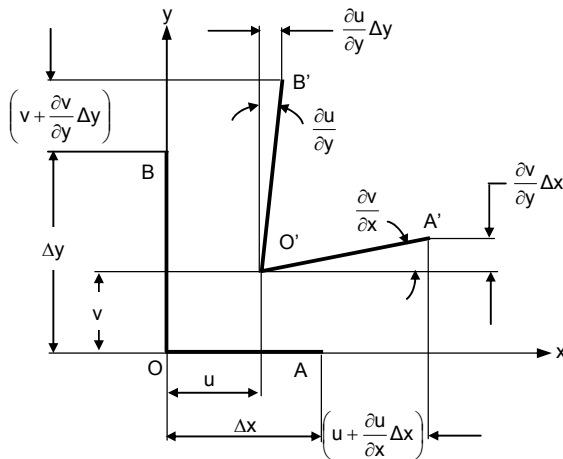


Fig. 1. Geometric representation of relations between displacements

The moiré fringe technique<sup>2,3</sup> is an experimental method to determine the components of displacement ( $u$ ,  $v$ ) or strain ( $\varepsilon_x$ ,  $\varepsilon_y$ ). On a part subjected to analysis, a grid of equidistant lines parallel to the  $y$ -direction is deposited by one of the methods described later. When a part is subjected to loads, deformation of the part, and consequently of the grid applied to it, occurs. The deformed grid is then superimposed on, and so compared to, a master or undeformed grid. The superimposition produces an optical effect (by mechanical interference), which produces the moiré fringes described by the following formula<sup>4</sup>:

$$I_m(x, y) = I_0(x, y) + b_1 \cos \left[ 2\pi \frac{u(x, y)}{p} + \alpha \right] + b_2 \cos \left[ 2\pi \frac{2u(x, y)}{p} + 2\alpha \right] + b_3 \cos \left[ 2\pi \frac{3u(x, y)}{p} + 3\alpha \right] + \dots = I_0(x, y) + \sum_{k=1}^K b_k \cos k \left[ 2\pi \frac{u(x, y)}{p} + \alpha \right] \quad (2)$$

where:  $I_0(x, y)$  is the background intensity variations,  $k_i$  and  $b_k$  describe the profile of the moiré fringes (using Fourier notation) and  $\alpha$  is the shift of the fringes,  $p$  is the pitch of the specimen grid.

This equation represents a continuous relationship between intensity and displacement that forms the basis for manual and digital analysis of moiré fringes. For the sake of simplicity, a transparent part having a set of parallel black lines applied to its surface is considered. If a master having an identical set of lines is placed directly on top of the part before the part is deformed, the density of lines is the same on the master and the part. With the aid of transmitted light, the master can be so placed that when the lines coincide, maximum transmission is observed, and when the lines of the master fall between the lines on the part, maximum darkness is observed. The relative positions (defined by parameter  $\alpha$ ) of the model and master grids is not important so long as a uniform light intensity is maintained.

Suppose the master is aligned so that maximum light is transmitted (lines coincide,  $\alpha = 0$ , Fig.2a). Now when the part is subjected to forces, strain occurs and the density of the lines on the part changes. Thus, in some areas the lines of the part and the master will coincide (maximum transmission), while in other areas, the lines of the master will fall between the lines of the part (maximum darkening or formation of a fringe). Now, at any point on the part, the strain can be calculated by simply measuring the distance between two consecutive fringes and dividing the pitch of the grid (distance from line to line) by this distance (Figure 2b).

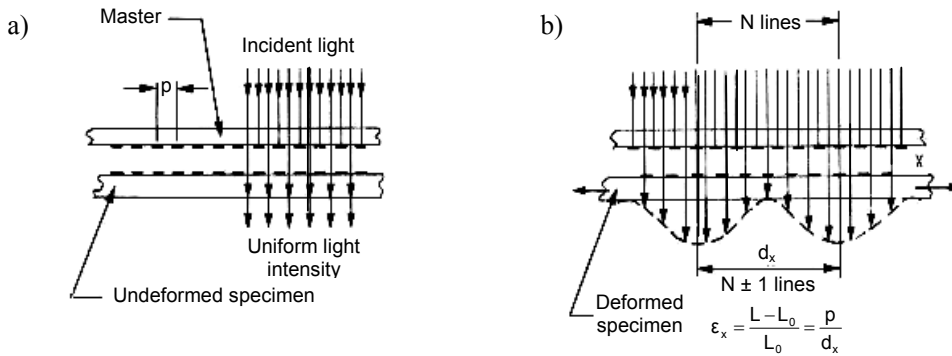


Fig 2. Scheme representing formation of moiré fringes: interaction of master and a) undeformed, b) deformed specimen grid.

Note also that the moiré fringe is a *line of constant displacement*  $u$  (or  $v$ ), and the overall moiré pattern is therefore a map of constant displacement contours<sup>5</sup>. Along a fringe we have  $u = \text{constant}$ , and the difference in the  $u$  value between two consecutive fringes is  $\Delta u = p$ . The complete picture observed is basically a tracing of the function  $u(x,y) = C$  with the value of constant  $C$  increasing or decreasing from one fringe to the next by the pitch,  $p$ .

## 6. Apparatus

As described in Section 5 the basis for the moiré fringe technique is the superposition of a reference (master) grille RG onto a modulated (deformed) grid SG.

The different optical arrangements that are available can be divided into two groups:

- physical superposition of grids (Fig.3a),
- superposition of grids by projection (Fig.3b-c).

Different optical arrangements can be used to record moiré patterns as shown in Fig.3.

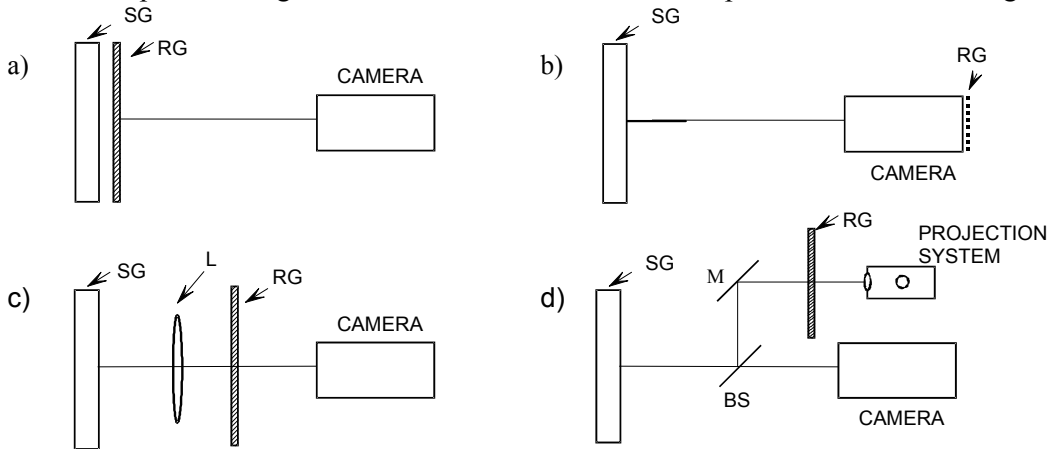


Fig. 3. Different optical arrangements used to generate moiré patterns: a) physical superimposition and b), c), d) configurations using projection to achieve superimposition of grids; RG – reference grille/grid, SG – specimen grid.

## Physical superposition of grids

This is the most obvious method, in which an undeformed master grille is laid directly onto a deformed specimen grid thus producing moiré fringes, which are then recorded by a camera (Fig.3a). This has the benefit of removing the need to resolve individual lines, so that the observer may, stand well back, and so be able to view a reasonably large area <sup>6,7</sup>. Problems with physical superimposition in this way are that out-of-plane movements will produce apparent in-plane deformation and that diffraction effects place a limitation on the fineness of the pitch that may be used, particularly when working in reflection, when the light has to pass back through the analyser from the specimen. Another factor, generic to all systems, is that it is necessary either to be fastidious in producing the specimen grid such that it is of good regularity (i.e. very sparse fringes when undeformed) or to record ‘zero-field’ fringes and perform a subsequent subtraction of the initial spurious displacement fields from those observed under load. This is not a great problem with modern computerised systems, but too many ‘zero-field’ fringes can render it difficult to appreciate in real-time what is happening. Due to the physical contact between grids it is sometimes difficult to introduce the phase shift required for fringe pattern analysis.

## Superposition of gratings by projection

With relatively coarse gratings, it is feasible to project the reference grating on to the specimen one using an imaging system (Fig.3d), or to project an image of the specimen onto the reference (Fig.3b,c). These methods have the feature that by defocusing the lens, or using a small aperture, the projected artefact contains effectively no harmonic of the grating higher than the first, so that the simpler algorithms of fringe pattern analysis may be employed. The difficulty is that non-flatness of the specimen, or distortions due to lens aberrations, will cause errors that are not obvious. It is of some importance to use a rigid set-up, as any instability in the connection between the two gratings will result in movement of the fringes. On the other hand this effect may be used for implementing the temporal phase shifting method <sup>8</sup>. In these arrangements it is relatively easy to introduce phase-shift by moving the reference grating in the direction perpendicular to its lines.

## 7. Sample preparation

### 7.1 Amplitude grids technology

For the application of geometric moiré, grids (bi-directional periodic line structures) of relatively large pitch have to be attached to the specimen by one of a variety of processes. To do so the master grating has to be available <sup>2,6</sup>. Pitches of master gratings used for geometrical moiré vary from 1 mm to 10  $\mu\text{m}$  (i.e. 1 to 100 lines per mm).

The coarse gratings, 1 to 5 lines/mm, can be obtained from graphics arts suppliers, in sheets of 25 by 50cm. Commercial artists use both cross-gratings and one-way gratings, of various line densities, for shading. The cross-gratings are often rectangular dot arrays. Finer gratings (5 to 10 lines/mm) are available from high quality lithographers or photoengravers and their suppliers. A few suppliers have gratings with frequencies greater than 40 lines/mm. Optical grating companies supply gratings beyond 40 lines/mm. Suppliers to the stress analysis industry provide 20 to 40 lines/mm rulings and cross gratings, on glass, up to 20 by 25 cm, as well as metallic dot arrays of 20 lines/mm. Most commercial gratings have a line width of approximately 50% of the pitch, which is optimum to achieve maximum fringe contrast.



Photography can be used to duplicate gratings and in special cases to vary line width, by varying exposure and developing times.

Once in possession of a master grating, it has to be attached or replicated at the specimen surface <sup>7</sup>. A technique which is common for producing a specimen grid is "stripping film", in which the black/white dots (cross pattern) are photographically reproduced from "master" grids in which the halide emulsion is carried on a duplex backing. Material is made to adhere to the specimen surface with glue, with the antihalo layer outward. This is then peeled off, leaving the grid on the specimen. A fairly smooth and clean surface is generally desirable for good results. A similar concept to the "stripping film" lies behind commercially available "nickel dot" grids separable from a steel backing sheet. Black epoxy is generally used as the transfer medium, leaving reflective dots at the black background. For high temperature applications a white ceramic cement is preferred: the nickel turns dark as it oxidizes, giving a reverse contrast.

Soft or elastic materials require the pattern application without any supportive layer. Such an application can be realized by stencilling through a fine nickel mesh with an array of holes of up to 80 holes/mm. The mesh is temporarily fixed and properly oriented to the surface by using a non-drying adhesive. After drying, the surface is sprayed with a white pigment e.g. titanium dioxide, which is recommended for both ambient and high-temperature applications. For very large (percentage) strains, or for large fields of view, a quite mundane process with large dots is possible e.g. printing with an etched roller or a use of an adhered simple woven textile or wallpaper with a stripe. For the pitch values in the range 2.5 to 6 dots/mm, ink-printed and litho copies of a negative called a "film tint", on sheets of paper, are commercially available. These printed-paper patterns can be fixed to the objects (usually large engineering structures such as houses and bridges) using standard paper-hanging paste. Table 7.1 summarizes the available methods for producing amplitude specimen grids as a function of the material of the object being measured <sup>7</sup>.

Table 7.1 Specimen grating patterns associated with different material <sup>7</sup>

Metals	Masonry	Plastic, composites	Others
Non-ferrous 1-4 Steel 1-4	Concrete 1-3, 6 Brick, 1,2, 6 Timber, 1, 2 Clay 4	PCV, 4 Carbon fibre, 4 Rubber, 4, 6	Textiles, 5 Graphite, 4 Skin 3 Card 3
1, Printed paper patterns; 2, "Stripping film"; 3, Direct printing; 4, Stencilled patterns; 5, Untreated materials; 6, Other: textile, random patterns with tuned imaging optics.			

## 7.2 Master grids

Two types of masters are available for use with transferable moiré grids:

1. Master grilles – uni-directional lines,
2. Master grids – bi-directional lines.

When used in conjunction with a specimen grid, superposition of a master grille will show u and v displacement fringes independently, depending on the grille line orientation with respect to the bonded grid lines. On the other hand, a master grid, superimposed over a bondable grid, will show both the u- and v-displacement fringes simultaneously.

Typical masters are available in line densities 8, 20, 40 lines per mm. The lines are deposited on a 1.5 mm glass plate, and are available in sizes: 100mm x 100 mm or 25.4mm x 25.4 mm. Other frequencies of master grilles or grids may be ordered from a variety of companies.



## 8. Calibration procedure

Prior to the measurement the following parameters should be known and/or determined and properly set:

- the period and quality of the specimen and master grids ,
- the magnification and quality of the imaging optics.

In the case of commercial grids used for replication at the specimen, the producer guarantees and gives information about the grid period and its quality which should be not worse than 1/10-1/20fringe within the measurement area. The quality of grid replication at the specimen should be checked by observation of “moire fringes” occurring between the specimen grid (while no load is applied) and the master grille. If no fringes appear in the required field of view the grid replication process is correct.

The quality of the imaging optics should be assured by the producer, however in the case of laboratory set-ups, or after any changes in the commercial system, this parameter should be checked. It is easy to do with the help of unloaded specimen grid and master grille. Placing them into one of the set-ups shown in Fig.3 we should get so called “null fringe field” i.e. there should be no fringes at the output of the system. If more than one fringe appears the imaging system should be corrected by the producer.

In general the set-up in its initial state i.e. the nonloaded specimen grid compared with the master grille should not produce moiré fringes in the measurement field of view. If there are fringes, they may be caused by:

- mismatch of the period or orientation between specimen and master grids. In the latter case linear fringes are obtained and they may be removed by changing the relative angular position between the grids. However if a period mismatch between grids occur, it introduces constant carrier linear fringes in the moiré fringe pattern. These carrier fringes are often introduced in purpose in order to facilitate the analysis of the fringe pattern.
- errors in the specimen grid due to its bad quality, or influence of the aberration in the imaging optics.

If just a single fringe (or quasilinear carrier fringes) appears, the initial (so called “zero”) fringe pattern is captured and the initial displacement field is calculated ( $u_i(x,y)$  or  $v_i(x,y)$ ) and stored in computer memory. During measurements these values are subtracted from the actual result and in this way this group of systematic errors are eliminated.

The calibration of the optical magnification is done by taking an image of an object of known dimension in the focal plane of the camera and associating the pixels on the camera to appropriate points on the object. The magnifications in  $x$  and  $y$  directions are calculated as:

$$\beta_x = \frac{\Delta x \cdot k_x}{d_x} \quad \text{and} \quad \beta_y = \frac{\Delta y \cdot k_y}{d_y} \quad (10)$$

where:  $k_x$ ,  $k_y$  are the actual number of pixels for the object dimensions  $d_x$  and  $d_y$  in  $x$  and  $y$  directions.

The global verification of these settings can be achieved experimentally by a calibration specimen of known geometry such as a beam subjected to four-point bending and a disc subject to compression across the diameter or a tensile strip. The exact circumstances of the component test must be reproduced including its geometry, material constants, temperature and loading conditions.



## 9. Recording and measurement procedures

The measurement procedure in-plane displacement/strain by geometric moiré consists of the following steps:

1. Preparation of the sample by introducing a specimen grid at its surface
2. Attachment of the sample to the load unit
3. Alignment of the measurement set-up towards the sample with special attention focused on the relative alignment of the master grille towards specimen grid (for horizontal grating). The imaging system should be perpendicular to the surface of the sample with the grid. The sample should be placed in the front focal plane of the imaging optics.
4. Ensure that no unforeseen relative movement of the measuring set-up with respect to the sample occurs.
5. Determine the magnification of the imaging system.
6. Identify the area of interest
7. Adjust the intensity of the sample illumination; no saturation on the CCD should occur and the full dynamic range of the camera should be used.
8. Capture the initial set of fringe patterns, and calculate the initial displacement fields, when the sample is under no load or under initial load.
9. Run the series of measurements. Ensure that the fringe density is not too high i.e. that the fringes are all time resolved by the CCD camera.
10. Repeat points 3,4,8,9 for the master grille located in the vertical direction.
11. Evaluate the results and correct them by subtracting the initial displacement maps.
12. Calculate strain using the proper magnification and the selected length of differentiation.

The measurement may be performed with a grid master in which case two simultaneous moiré patterns are observed and recorded by photographs or CCD camera. However, this procedure is preferred primarily in dynamic testing due to more complicated fringe pattern analysis procedures.

## 10. Data processing procedures

As the result of the measurement procedure, the sets of moiré fringe patterns are captured. The moiré fringes contain encoded information related to the displacement. The fringes may be analysed manually<sup>1,3,4</sup> and sometimes for a quick check of the obtained values of strains this manual procedure is still applied. However due to the digital character of the data captured by the CCD or CMOS camera, automatic fringe pattern analyses are widely used in most of the commercial and laboratory systems.

### 10.1 Manual analysis

The example in Figure 4<sup>1</sup> will clarify the general procedure for classical (manual) measurement and use of moiré patterns. For simplicity, suppose that a grid is applied to the part and the master used for analysis is a grille. The direction perpendicular to the lines of the master is designated “x”. After application of a load, a pattern of moiré fringes is observed. Those fringes represent a map of



the displacement in direction  $x$ , or a map of “ $u$ ”. An arbitrary line traced in direction  $x$  will yield  $u(x)$  along this line. Consequently  $\epsilon_x$  can be measured at any point as the slope of  $u(x)$ .

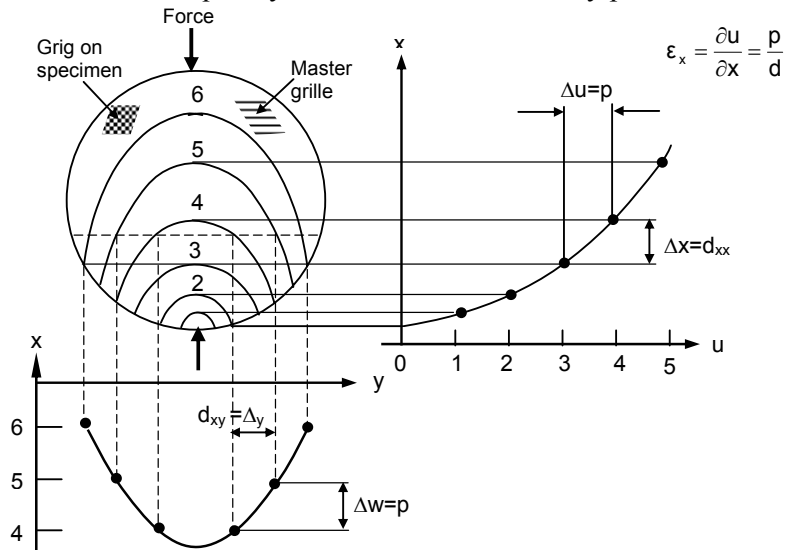


Fig. 4. Procedure of manual analysis of moiré fringes for the example of a compressed disk [TN-703].

Now, if the master grille is rotated  $90^\circ$ , a new set of moiré fringes will appear that represents a map of the displacements in direction  $y$ , or a map of  $v$ . Thus, the two patterns give the complete solution at every point since we now have:

$$\epsilon_x = \frac{\partial u}{\partial x} = \frac{p}{d_{xx}} \quad \epsilon_y = \frac{\partial v}{\partial y} = \frac{p}{d_{yy}} \quad \gamma_{xy} = \frac{\partial u}{\partial y} + \frac{\partial v}{\partial x} = \frac{p}{d_{xy}} + \frac{p}{d_{yx}} \quad (11)$$

The moiré fringe pattern can be modified<sup>3,5</sup> by:

- rotation of the master,
- mismatch between specimen grid and master.

Uncontrolled modifications<sup>8</sup> may be a source of errors in measurement and strain calculation. On the other hand, considering a rotation of the master with reference to the specimen grid, it can be shown that if the moiré fringes at a particular point move in the same direction as the applied rotation (fringes move clockwise when master is rotated in a clockwise direction), that indicates that the part being analysed is experiencing tensile strain. If the moiré fringes move in the opposite direction to the rotation (fringes move counterclockwise when the master is rotated in a clockwise direction), then it indicates that the part being analysed is strained in compression. In this way the sign of strain may be manually determined. The technique of a mismatched master is normally used to improve the sensitivity at low levels of deformation by providing a larger number of data points for manual analysis, and by decreasing the gauge length of measurement.

## 10.2 Digital analysis

Digital geometric moiré<sup>4,8</sup> involves the use of digital images for determination of 2D in-plane displacement maps and for strain calculations. The light intensity captured for vertical master

grilles is represented by Eq. 2. However, considering only the first two terms, the intensity of moiré fringes becomes:

$$I_m(x,y) = I_0(x,y) + b_I \cos\left[\frac{2\pi u(x,y)}{p} + \alpha\right] \quad (12)$$

If a grating with horizontal lines is applied the intensity  $I(x,y)$  is related in an equivalent way to the  $v(x,y)$  displacement field.

The moiré fringes given by equation (12) may be modified by:

- changing the relative phase  $\alpha$  by translating one of the gratings in the direction perpendicular to the grating lines. In such a case the  $i$ -th intensity pattern is described as:

$$I_{mi}(x,y) = I_0(x,y) + b_I \cos\left[2\pi \frac{u(x,y)}{p} + \varphi_i'\right] \quad (13)$$

where  $\varphi_i' = \alpha + \varphi_i$ , where  $\varphi_i$  is the phase shift introduced by linear shifting of the master grille

- introducing a spatial carrier frequency into the moiré pattern by superposition of gratings with slightly different pitches  $p$  and  $p'$  (pitch mismatch) or setting an angle  $\theta$  (rotation mismatch) between the reference and deformed gratings. In such a case the equation of moiré fringes is given by:

$$I_m(x,y) = I_0(x,y) + b_k \cos k \left[ 2\pi \frac{u(x,y)}{p} + 2\pi f_{ox} x \right] \quad (14)$$

where  $f_{ox}$  is the spatial carrier frequency in the  $x$  direction (of course this frequency may be introduced in an arbitrary direction).

The goal of digital analysis of moiré fringes is to decode the displacement function ( $u(x,y)$  or  $v(x,y)$ ) from the two-dimensional intensity distribution  $I(x,y)$  at each sampling point. The parameters  $\phi_i$  and  $f_{ox}$  are required for the application of one of the automatic fringe pattern analysis methods<sup>9,10</sup>:

- **temporal** phase shifting method, TPS, in which at least 3 fringe patterns with phase shifts have to be captured. This method is used for the analysis of static phenomena, and capturing data in stable conditions.
- **spatial** carrier phase shifting method, SCPS. Here a single fringe pattern with spatial carrier fringes is required for displacement analysis. This method is usually used for the analysis of dynamic phenomena.

The Fourier transform method, FT, which also requires a single fringe pattern for full analysis can also be used for the analysis of dynamic phenomena. However it creates significant errors at the edges of the domain (sample discontinuity)<sup>10</sup>, so FT is not usually used for experimental mechanics applications.

The main stages of fringe pattern(s) analysis leading to in-plane displacement and strain maps include:

- calculation of phase  $\text{mod}(2\pi)$  by one of the phase measuring methods,
- phase unwrapping,
- phase scaling (displacement maps determination),
- strain calculation.



### 10.2.1 Phase modulo $2\pi$ determination

The value directly related to displacement is the local phase of the quasi-cosinusoidal fringes in the moiré fringe pattern (Eqs.2 and 12). However this value is screened by local variations in background ( $a(x,y)$ ) and the contrast of the fringes ( $b(x,y)$ ), therefore in order to solve this problem two alternative approaches are employed.

**Temporal phase shifting method** is based on the reconstruction of the phase  $\phi(x,y)$  from a number of fringe patterns (Eq.13) which differ from each other by various values of a discrete phase shift  $\varphi_i$ .

where  $\varphi_i = (i-1)\varphi_0$  and  $i=1\dots M, M \geq 3, \varphi_0 = 2\pi/M$ .

In general only three intensity measurements are required to calculate phase from Eq. 12. However this solution requires very accurate calibration of the phase-shifter device to ensure a defined amount of phase shift, and capturing intensity data without any nonlinearity (which is not true for moiré fringes). This difficulty may be overcome by increasing the number of frames and by applying a so-called (M+1) algorithm<sup>9</sup>. The most popular algorithm is the five intensity self-calibrating algorithm with  $\varphi_0 = \pi/2$ . It minimizes the influence of linear errors in phase shifting and the second order nonlinearity of the captured image intensities. In this case the phase is calculated according to the equation:

$$\phi'(x, y) = \arctan \frac{2(I_2(x, y) - I_4(x, y))}{2I_3(x, y) - I_5(x, y) - I_1(x, y)} \quad (14)$$

where  $\phi'$  is wrapped phase i.e. phase mod( $2\pi$ ).

If higher order nonlinearities are expected in the moiré fringes it is advisable to apply six- or even seven-frame algorithms<sup>11</sup> to compensate for this error.

The TPS method requires stable conditions during the time of capture of the set of fringe patterns needed for the calculations. For this reason TPS can be applied to the investigation of static events and in stable conditions (i.e. no vibrations and no significant environment condition changes).

**Spatial carrier phase shifting method** is based on the reconstruction of the phase  $\phi(x,y)$  from a single fringe pattern with linear carrier fringes<sup>4,12</sup>. The intensity captured is described by Eq.14. The SCPS method is based on a similar concept to the TPS, however the phase at a given point is calculated based on the intensities of neighbouring points. In SCPS a proper relation between the sampling frequency of the detector ( $f_d = 1/K$ , where  $K$  is the number of sampling points in the image) and the spatial carrier frequency,  $f_{ox}$  ( $f_{oy}$ ), has to be fulfilled in order to provide the chosen phase shift  $\varphi_0$  between sampling points (e.g. if  $\varphi_0 = \pi/2$  then  $f_{ox} = 1/4K$ ). For similar reasons as in TPS the most popular algorithm for the calculation of phase mod  $2\pi$  is the 5-point algorithm with a  $\pi/2$  phase shift between pixels. The SCPS method is widely used for automatic analysis of fringe patterns captured during dynamic processes and when measurements are performed in unstable conditions. In order to avoid higher order nonlinearities in the image, a slight defocusing of moiré fringes is often applied.

### 10.2.2 Phase unwrapping and scaling



The unwrapping or demodulation of the wrapped phase (phase  $\text{mod}(2\pi)$ ) creates a continuous phase field:

$$\phi(x, y) = \phi'(x, y) + N(x, y) \cdot 2\pi \quad (15)$$

where  $N(x, y)$  is the integer number of the fringe at the point  $(x, y)$  in the domain.

Unwrapping algorithms are necessary to remove phase jumps from the fringe distributions. Depending on the quality of the phase  $\text{mod}(2\pi)$  maps and the fringe pattern domain, several algorithms are available<sup>10,11</sup> including:

- line-by-line scanning ( for  $x$  and  $y$  direction) which is used when the quality of the fringes is very high. It fails when noise and domain discontinuities exist.
- spanning tree algorithms which check the phase difference between a central pixel and its neighbours and chooses the route with the minimum gradient. An attractive approach uses the amplitude of each pixel as a criterion to walk through the phase map (maximum cross amplitude spanning tree). This is the most popular algorithm for maps of standard quality due to both its speed and the quality of the results.
- a modulation queuing algorithm which utilises a so-called “quality map” which is defined by local modulation and phase  $\text{mod} 2\pi$  gradient values. This algorithm is used for noisy patterns and interferogram domain with complex shape.
- temporal unwrapping which utilizes consecutive phase  $\text{mod} 2\pi$  maps to determine the actual number of a fringe  $N(x, y)$ .

After calculating the continuous phase map with proper values and sign, it is transformed to in-plane displacement maps according to the relations:

$$u(x, y) = \frac{p\phi_x(x, y)}{2\pi} \quad \text{and} \quad v(x, y) = \frac{p\phi_y(x, y)}{2\pi} \quad (16)$$

### 10.2.3 Strain calculation

If the displacement fields  $(u(x, y), v(x, y))$  are known, it is possible to calculate the strain field for the specimen under load. In practice it is realised by differentiation of the displacement data. The in-plane strains are calculated according to the relations:

$$\varepsilon_x = \frac{\partial u}{\partial x} = \frac{u_{i+n} - u_{i-n}}{2n\Delta x'} \quad (17)$$

$$\varepsilon_y = \frac{\partial v}{\partial y} = \frac{v_{i+n} - v_{i-n}}{2n\Delta y'} \quad (18)$$

$$\gamma_{xy} = \frac{\partial u}{\partial y} + \frac{\partial v}{\partial x} = \frac{u_{i+n} - u_{i-n}}{2n\Delta y'} + \frac{v_{i+n} - v_{i-n}}{2n\Delta x'} \quad (19)$$

where:  $\Delta x' = (1/\beta_x)\Delta x$  and  $\Delta y' = (1/\beta_y)\Delta y$

$\beta_x, \beta_y$  - imaging system magnification,

$\Delta x, \Delta y$  - distance between neighbouring pixels at CCD matrix plane,

$2n$  - number of pixels over which differentiation is performed.



### 10.2.4 Additional digital data processing

The digital nature of the data used in sequential stages of fringe processing makes it possible to modify the data, enhance its quality and calculate related physical quantities. The possible data processing operations include, but are not restricted to:

- *reference displacement field subtraction*. The displacement map obtained for the given loading conditions contains information about the displacement under investigation and also about the total systematic error which may include: specimen and reference grid imperfections, optical system aberrations, initial rotation of the grids etc. In digital geometric moiré this systematic error may be easily removed by using a reference map. This map is calculated from moiré fringes captured when a specimen is under an initial load (so called “zero displacement map”). When the reference map is subtracted from the actual displacement map, the final map includes information only about the real displacement of the sample. This is true if the optical set-up in which the fringes are captured is exactly the same in both loading cases.

- *filtering*. Very often a fringe patterns and/or phase map are subjected to severe high frequency noise which degrades the quality of the final displacement and strain maps. For this reason the data (at various stages of processing) are filtered with a low pass filter, which removes the noise. However such filters have to be applied with great care as they can also modify the results significantly, especially if high gradients are present in the displacement or strain maps.

- *masking*. One of the steps in the reconstruction process is to mask those areas which do not belong to the fringe pattern domain. The mask is also implemented in areas where the fringe contrast is low, or the level of noise is too high. The provision of a mask in this area allows calculations to be performed only in the areas with appropriate intensity values and therefore avoids errors during data processing.

- *arithmetic and logical operations*. Various calculations on an image or group of images (intensities, phases, displacements) can be performed. The most popular operations on images and phase maps are: summation, subtraction, difference, multiplication, calculation of RMS, minimum and maximum value etc. These operations allow values such as shear strain or material constants (Poisson ratio, Young modulus etc.) to be calculated.

## 11. Accuracy and sensitivity

Accurate results can be obtained by using accurate grids and masters where such issues as:

- uniformity of the pitch “ $p$ ” throughout the grid,
- absolute accuracy of the pitch,
- contrast of the edges of the lines,
- imaging conditions,
- proper transformation of the object in-plane displacement into the grid deformation etc.

are extremely important. However if digital moiré fringes analysis is performed, the measurement accuracy depends also on the accuracy of the algorithm applied for processing the fringes. The typical accuracy of temporal phase shifting algorithm is pitch/40, while for spatial carrier phase shifting algorithm it is pitch/20.

The basic sensitivity of the measurement is affected by:

- the pitch “ $p$ ”,
- the contrast of the moiré pattern, which is in turn a function of the grid design,
- the resolution of the detection system (CCD or CMOS cameras).



For example, when using a grid with a pitch equal to  $p = 0.025$  mm (40 lines/mm) and assuming a moiré fringe distance of 25mm covering the field of view of the imaging system, the strain calculated in the traditional (manual) way (pitch divided by fringe distance) is

$$\varepsilon_x = \frac{p}{d} = 1000 \text{ } \mu\text{m/m}$$

However if digital phase analysis is applied for determination of the in-plane displacement it is not necessary to have a full moiré fringe in the field of view and it is easy to detect a displacement which is represented by 1/20th of moiré fringe i.e.

$$\varepsilon_x = \frac{p}{20d} = 50 \text{ } \mu\text{m/m}$$

Clearly, the sensitivity is directly related to the capability of the measurement system to detect in-plane displacement within the considered field of view. Digital analysis is not restricted to the determination of moiré fringe extrema locations (as in the case of manual analysis) but it detects displacement at each sampling point individually. For this reason the sensitivity of geometric moiré supported by digital phase analysis is increased significantly.

## 12. Areas of applications

Obviously, the moiré fringe method of experimental strain analysis will be applied primarily to solve problems that cannot be solved easily, accurately or economically by other methods. Typical problems will include:

1. High-temperature measurements (heat treatments, welding, thermal stresses, etc.)
2. Measurement of large elastic and plastic strains without reinforcing effects in thin films, low-modulus materials, etc.
3. Two- and three-dimensional analysis of transparent models using the embedded-grid principle.
4. Absolute measurements of strain to establish properties of materials, long-term-stability measurements, etc.
5. Measurement of relatively big structures (civil engineering) over extended period of time.

## 13. Bibliography

1. Kobayashi, A.S., ed: *Handbook of Experimental Mechanics*, Prentice Hall, Inc., 1987.
2. Burch, J.M. and Forno, C., "A high-sensitivity moiré grid technique for studying deformation in large objects", *Opt. Eng.*, 14, 175-185, 1975.
3. Theocaris, P.S., *Moiré Fringes in Strain Analysis*, Pergamon Press, Oxford, 1969.
4. Durelli, A.J. and Parks, V.J., *Moiré Analysis of Strain*, Prentice-Hall, Englewood Cliffs, New Jersey, 1970.
5. Patorski K., *The Handbook of the Moiré Technique*, Elsevier, Oxford, 1993.
6. Weller, R. and Shepard, B.M., "Displacement measurement by mechanical interferometry", *Proc. Soc. Exp. Stress Analysis*, 6(1), 35-38, 1948.
7. Kafri, O. and Glatt, I., *The Physics of Moiré Metrology*, Wiley, New York, 1990.
8. Kujawinska, M., "Automated in-plane moiré techniques and grating interferometry" in "*Optical Methods in Experimental Mechanics*", Laerman K., ed., Springer, Wien, New York, 123-195, 1998.
9. Robinson, D.W. and Reid, G.T., *Fringe Pattern Measurement Techniques*, IOP Publishing Ltd., 1993.
10. Huntley, J.M., "Automated fringe pattern analysis in experimental mechanics: a review", *Journal of Strain Analysis*, 33, 105-125, 1998.
11. Kujawinska, M. and Wójciak, J., "Spatial-carrier phase-shifting technique of fringe pattern analysis", *Proc. SPIE*, 1508, 61-67, 1991.

